One-step synthesis of single-walled carbon nanohorns dispersed with Pd-Ni alloy nanoparticles by gas-injected arc-in-water method and effects of synthesis factors on their hydrogen sensor sensitivity

Noriaki Sano, Taiga Ishii, Hiroki Mori, Yusuke Ikeyama, and Hajime Tamon

Citation: Journal of Applied Physics **112**, 044301 (2012); doi: 10.1063/1.4745045
View online: http://dx.doi.org/10.1063/1.4745045
View Table of Contents: http://scitation.aip.org/content/aip/journal/jap/112/4?ver=pdfcov
Published by the AIP Publishing

One-step synthesis of single-walled carbon nanohorns dispersed with Pd-Ni alloy nanoparticles by gas-injected arc-in-water method and effects of synthesis factors on their hydrogen sensor sensitivity

Noriaki Sano,[a] Taiga Ishii, Hiroki Mori, Yusuke Ikeyama, and Hajime Tamon
Department of Chemical Engineering, Kyoto University, Kyoto 615-8510, Japan

(Received 25 January 2012; accepted 17 July 2012; published online 17 August 2012)

Single-walled carbon nanohorns (SWCNHs) dispersed with Pd-Ni alloy nanoparticles were synthesized in a technique requiring a single step by a gas-injected arc-in-water method using Pd-Ni-C mixed powders charged in an anode hole. It was found that the Ni/Pd weight ratio in the alloy nanoparticles dispersed in the products uniquely depended on the initial Ni/Pd weight ratio; Pd in the products was enriched by a factor of two when the Ni/Pd weight ratio in the initial mixture was higher than 0.1, while Ni was enriched at a Ni/Pd weight ratio below this threshold. The average diameter of alloy nanoparticles increased with the initial weight of the metallic components, while the average diameter of the discrete forms of the SWCNH aggregates exhibited the opposite tendency. Increasing the amount of the metallic compounds in the initial mixed powders caused the enrichment of Pd. The effect of adding Pd-Ni alloy nanoparticles into the products on the carbonaceous structures of SWCNHs was not detected by Raman analysis. The sensitivities of H_2 sensors using the SWCNHs dispersed with Ni, Pd, and Pd-Ni alloy nanoparticles were compared, and the sensitivity of the sensor using the Pd-Ni alloy was the highest. © *2012 American Institute of Physics*. [http://dx.doi.org/10.1063/1.4745045]

I. INTRODUCTION

Since single-walled carbon nanohorns (SWCNHs) were first synthesized,[1] their structural and physical properties have been intensively investigated because SWCNHs are expected to exhibit superior performance in various applications, including drug delivery, catalyst support, gas adsorption, and chemical sensors.[2–6] Methods for synthesizing SWCNHs have been developed in recent years so several approaches are currently known.[1,7–16] First, the method using laser ablation was reported to synthesize SWCNHs with high purity and yield.[1] Following this discovery, the methods using arc discharge were conceived.[7–16] These methods are considered superior in terms of their low cost because no expensive equipment such as a high power laser or vacuum system is required. In all of these methods, the reaction conditions with high temperature (above 5000 K) are utilized to vaporize graphite blocks. An exceptional new method to synthesize SWCNHs at 1327 K was reported very recently.[17] However, this method requires further investigation to raise the yield drastically for any use. In this work, the so-called gas-injected arc-in-water (GI-AIW) method,[4,7–9] which was developed by modifying a submerged arc discharge method,[8,16] was employed for synthesizing SWCNHs due to its simplicity and cost-effectiveness.

Carbon materials dispersed with metallic nanoparticles are preferable for use in catalytic reactions.[3,18,19] Pd dispersed on carbon materials is especially widely used in reactions with H_2.[18,19] In the present study, Pd dispersed in the SWCNH products was alloyed with Ni to improve its reactivity. Here, the GI-AIW method was employed to synthesize SWCNHs dispersed with Pd-Ni alloy nanoparticles in a single step. Conventional methods require two steps for the preparation of metal-dispersed carbon materials;[3,18,19] the first step is for the synthesis of carbon materials, and the second is for depositing metallic components thereon. The GI-AIW method is remarkable in that such a metal-loading step can be omitted, and the one-step synthesis to obtain metal-dispersed SWCNHs can be realized.[20,21] In this study, the Ni/Pd ratio and the amount of metallic components in the electrode components were varied to observe their effects on controlling the structures and components of the products. Prior to this observation, H_2 sensors using the SWCNHs dispersed with Ni, Pd, and Pd-Ni alloy nanoparticles were compared to confirm the superiority of alloying Pd with Ni.

II. EXPERIMENTAL

A. Synthesis of SWCNHs dispersed with Pd-Ni alloy nanoparticles

The electrode configuration used in the GI-AIW method to produce SWCNHs dispersed with Pd-Ni alloy nanoparticles is shown in Fig. 1. The cathode was made of graphite rod (diameter = 20 mm, length = 50 mm) that had a hole (diameter = 12 mm, depth = 25 mm) at its bottom to host the arc plasma. At the top of the cathode, four narrow holes were drilled to introduce N_2 into the arc plasma zone. The anode was made of graphite rod (diameter = 3.05 mm, length = 150 mm). A hole of 1 mm diameter was drilled along its axis to charge mixed powders of Pd (300 mesh), Ni (400 mesh), and C (8 μm diameter). The density of the charged-powder bed was approximately 1 g cm^{-3}. The weight ratio of Pd and Ni in the initial mixed powders charged in the anode hole was changed to observe its

[a]Electronic mail: sano@cheme.kyoto-u.ac.jp.

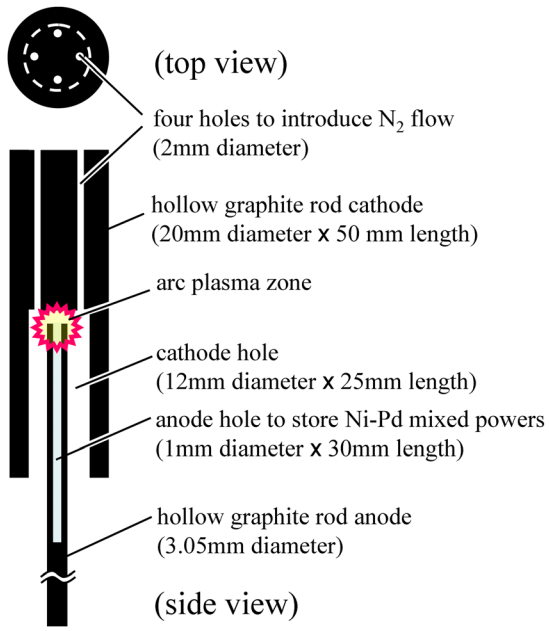

FIG. 1. Dimensions of graphite electrodes used in the present study.

influence. The details of the set-up to generate the arc discharge can be found in previous publications.[9,20] These electrodes were submerged in water, and the arc discharge was generated at the tip of the anode placed in the cathode hole. To continue the arc discharge, the anode was shifted up toward the static cathode at a constant speed of 1.5 mm s^{-1}. The carbon vapor generated by the arc discharge was carried by N_2 gas (5 l min^{-1}) to the surrounding water, resulting in rapid quenching at the 10^6 K s^{-1} level.[22] In such an environment, carbon vapor can be transformed to SWCNHs. Under these conditions, Pd and Ni were also evaporated together with carbon and were converted to alloy nanoparticles simultaneously with the formation of SWCNHs. As a result, SWCNHs dispersed with Pd-Ni alloy nanoparticles can be obtained from a one-step synthesis. The powdery products of the SWCNHs dispersed with Pd-Ni alloy were supposed to float on the water surface because of the hydrophobic character of their surfaces. Bulky deposits containing multi-walled carbon nanotubes were also formed simultaneously, and they partially remained inside the cathode hole or sank down to the bottom of the water container. This study focused on analyzing the floating products. When SWCNHs dispersed with Pd or Ni (not in alloy form) were synthesized for comparison, the powders of Pd or Ni mixed with C were charged in the anode hole in the arc discharge process.

B. Analyses on structures and components of the synthesized products

A transmission electron microscope (TEM) (JEOL, JEM-1010) with an electron energy of 100 keV was used to conduct structural observation and particle size analysis on the products. A field emission scanning electron microscope (FESEM) (JEOL, JSM-6701F) was also used to observe the products. An x-ray diffractometer (XRD) (Rigaku, RINT2100) with Cu Kα radiation under a power of 40 kV and 40 mA and Raman spectroscopy (Raman Systems, R-3000) at an optical wavelength of 532 nm were used to analyze the crystal structure of the products. An energy-dispersive x-ray analyzer (EDX) mounted on an SEM (Technex Lab Co., Tiny-EDX(LE)-α) was used to determine the Ni/Pd ratio in the alloy nanoparticles. A dynamic light scattering (DLS) (Otsuka Electronics, ELS-8010 M) was used to determine the particle size distribution of the discrete forms of the products in ethanol dispersed by a sonication bath (Velvo-Clear, VS-25) with a power of 25 W.

C. H_2 sensors using SWCNHs dispersed with Pd, Ni, and Pd-Ni alloy nanoparticles synthesized by GI-AIW method

In this study, H_2 sensors were fabricated using SWCNHs dispersed with the Pd, Ni, and Pd-Ni alloy nanoparticles. A photograph of the H_2 sensor is shown in Fig. 2 together with the set-up to observe its response to H_2. For fabrication of the H_2 sensor, a Pt film coating with a thickness of approximately 50 nm was applied to two areas of a glass plate by magnetron sputtering. The Pt films were connected to a high frequency inverter (TDK, Y-194 V-0) (40 kHz, 200 V_{p-p}) to generate dielectrophoresis[23–26] for trapping powdery SWCNHs to bridge between the Pt films. For this dielectrophoretic manipulation, SWCNHs were dispersed in ethanol and dropped on the trapping zone between the Pt films. This

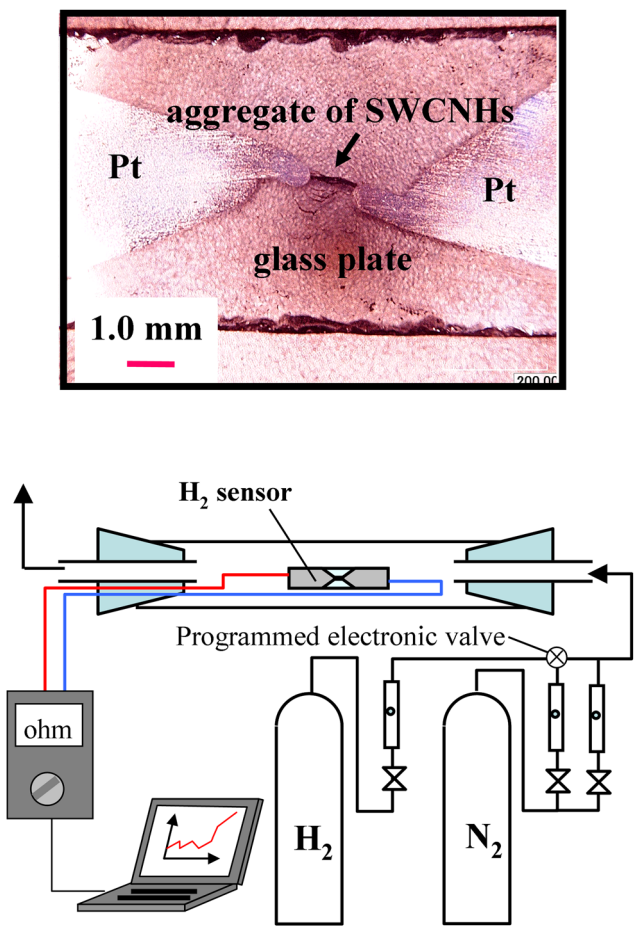

FIG. 2. A photograph of H_2 sensor using SWCNHs and the set-up to detect H_2 using this H_2 sensor.

H_2 sensor was placed in a glass tube and the Pt films were connected to a recordable digital multimeter (SANWA, PC5000) to monitor the ohmic resistance of the SWCNH aggregate bridging between the Pt films. The ohmic resistance of the Pt films was negligible compared with that of SWCNH aggregate so that the ohmic resistance monitored by the multimeter was governed by that of the SWCNH aggregate. It can be expected that the ohmic resistance of the SWCNH aggregate having Pd nanoparticles may be changed by supplying H_2 gas due to the interaction between Pd surface and H_2.[27] In this study, the initial value of the ohmic resistance was controlled to be approximately 150 kΩ by adjusting the amount of SWCNH powders in all conditions. In the glass tube, N_2 and N_2-H_2 mixture (H_2 concentration = 10%) were alternated in feeding at a flow rate of 370 cm^3 min^{-1} (flow velocity = 5 cm/s) at atmospheric pressure and room temperature. We set the duration for N_2 flow to 255 s and for N_2-H_2 flow to 45 s to alternate repeatedly in the gas feed. The sensitivity of SWCNHs dispersed with Pd-Ni alloy particles to H_2 was compared with that of SWCNHs dispersed with Pd or Ni.

III. RESULTS AND DISCUSSION

A. Microscopic observation on Pd-Ni alloy nanoparticles dispersed in the products

Fig. 3 shows examples of two TEM images and a FESEM image. The TEM images were obtained from the products synthesized at a Ni/Pd weight ratio of 1.0, for two different weight ratios of the metallic components in the initial Pd-Ni-C mixed powders charged in the anode hole. (The low magnification image (a) is for a weight ratio of 0.28, and the high magnification image (b) is for a weight ratio of 0.07.) In these TEM images, one can see that the metallic nanoparticles whose diameters are less than 20 nm seem to be highly dispersed in the SWCNH matrix. On the other hand, the carbonaceous parts of the SWCNHs seem to be aggregated together. It is known that Ni can be a catalyst to grow single-walled and multi-walled carbon nanotubes (SWCNTs and MWCNTs).[28–30] Nevertheless, SWCNTs and MWCNTs were rarely seen in any of the products in the present study. It should be noted that the selectivity for producing SWCNTs and MWCNTs in the syntheses using arc discharge in liquid should depend on the concentration of the catalytic metals in the reaction field.[31] In the reaction field in the present study, the concentration of Ni was considered to be excessive so that the production of SWCNTs and MWCNTs could be reduced to a negligible level. In the FESEM image of Fig. 3(c), one can see the nearly spherical shapes of aggregates of carbonaceous horns in SWCNHs. Each horn cannot be resolved in this image due to the ability of the present FESEM.

The diameter distributions of the metallic nanoparticles were obtained by the TEM observations. Fig. 4 shows the particle size distributions obtained from three weight ratios of metallic components in the initial Pd-Ni-C mixed powders (54.5%, 28.6%, and 7.4%). Here, the Ni/Pd weight ratio was constant at 1.0. It can be observed that the increase of the weight ratios of the metallic components lead to the increase

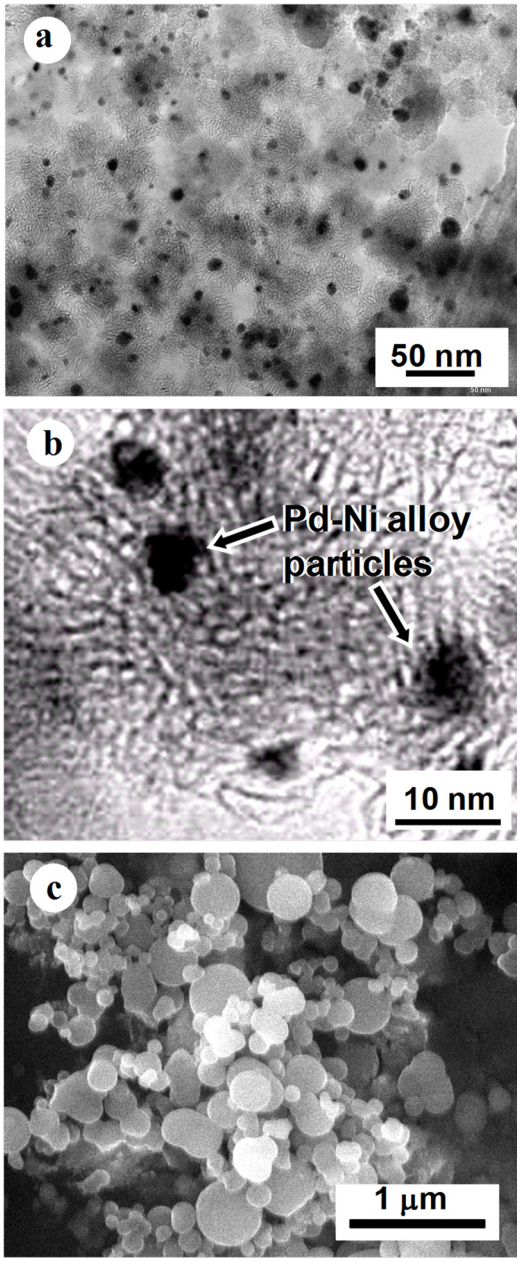

FIG. 3. TEM images of as-grown SWCNHs dispersed with Pd-Ni alloy nanoparticles synthesized at the Ni/Pd weight ratio 1.0 for two ratios, (a) 0.28 and (b) 0.07, of the metallic components (Pd and Ni) in the initial Pd-Ni-C mixed powders charged in the anode hole. SEM image, (c), of as-grown SWCNHs dispersed with Pd-Ni alloy nanoparticles synthesized at the Ni/Pd weight ratio 1.0 for a ratio of 0.20 of the metallic components in the initial Pd-Ni-C mixed powders.

of the average diameter of the metallic nanoparticles. It can be also noticed that the size distribution became broader when the weight ratios of the metallic components was increased. The trend in which the larger metallic ratio in the initial mixed powders causes larger final particle sizes can be explained by the growth rate of the metallic nanoparticles while they were solidified in the N_2 flow through the cathode hole. From the N_2 flow rate through the cathode hole, the reaction temperature, and the volume of the inter-electrode space, the resident time of the N_2 gas in the cathode hole would be at the level of 2×10^{-3} s.[22] In such a short time interval, the final particle sizes should tend to be larger when

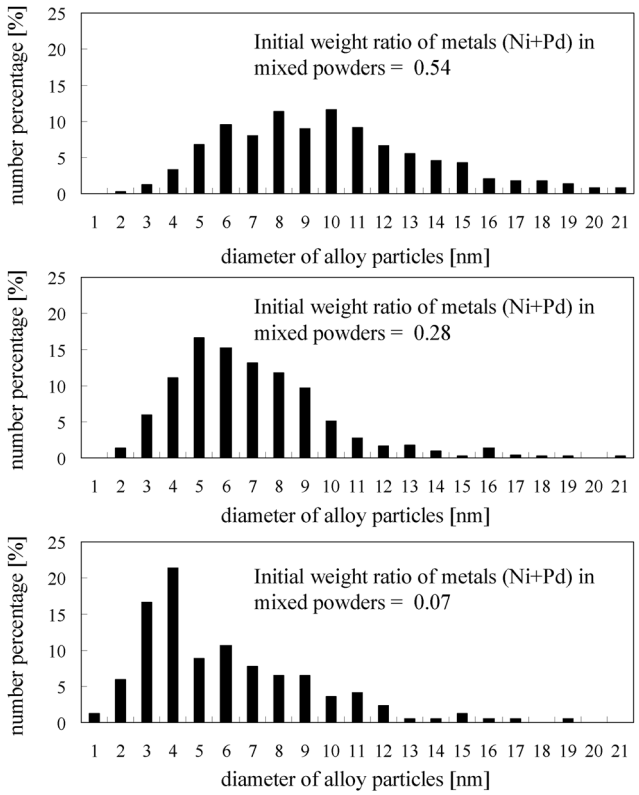

FIG. 4. Particle size distribution of alloy nanoparticles dispersed in the products synthesized at Ni/Pd weight ratio 1.0 for three ratios of the metallic components (Pd + Ni) in the initial Pd-Ni-C mixed powders: 0.54, 0.28, and 0.07. These particle size distributions were obtained by TEM observations.

the relevant growth rate is enhanced by increasing the concentration of the metallic components in the reaction field.

B. Analyses on metallic nanoparticles by XRD and EDX

Fig. 5(a) shows the XRD patterns obtained from various Ni/Pd weight ratios with a constant Pd/C weight ratio in the initial Pd-Ni-C mixed powders. It has been reported that the Pd-Ni alloy should exhibit a peak at a position between the peaks of pure Ni and of pure Pd.[32,33] Qualitatively, the peak position of the Pd-Ni alloy should have a tendency depending on the Ni/Pd ratio in the alloy, in which the peak should shift toward the Ni peak when the Ni concentration is higher and should shift to the opposite end when the Pd concentration is higher.[33] Fig. 5(b) shows two peaks at 40.2 and 44.5 degrees for pure Pd and Ni, respectively. It is shown that the SWCNHs dispersed with metallic nanoparticles synthesized with Pd-Ni-C mixed powders can exhibit the XRD peaks in this angular range under all conditions. Therefore, the metallic nanoparticles existing in the products should be made of Pd-Ni alloy. There is an observable tendency of the position of the peak from the resulting Pd-Ni alloy to tend to shift toward the Ni peak when the initial Ni/Pd ratio increases. Therefore, the XRD analysis suggests that the increase of Ni in the reaction field can cause the increase in Ni content in the alloy nanoparticle products, qualitatively.

Quantitative information about the influence of the initial Ni/Pd weight ratio on the product components was

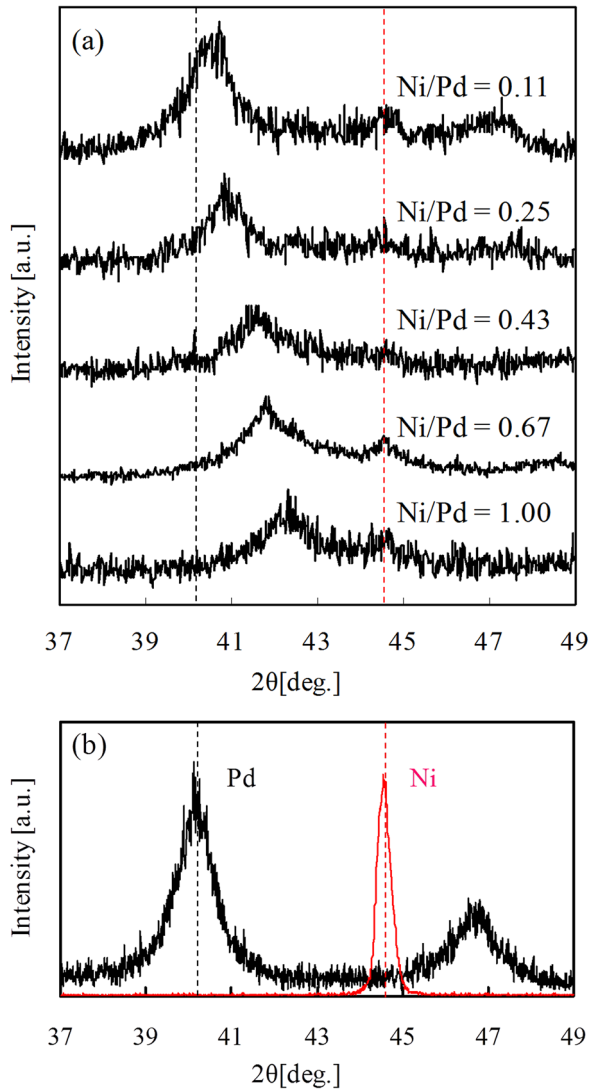

FIG. 5. XRD patterns of SWCNHs dispersed with Pd, Ni, Pd-Ni alloy nanoparticles synthesized at a Pd/C weight ratio 0.2 for various Ni/Pd weight ratios.

obtained by EDX analysis. As a result, there was discrepancy between the initial Ni/Pd weight ratio and the Ni/Pd weight ratio in the products. This result suggested that when one wants to obtain a product which needs a specific Ni/Pd weight ratio, the initial Ni/Pd ratio should be carefully chosen because the Ni/Pd ratio in the products should change from the initial Ni/Pd ratio.

Fig. 6 summarizes the results by EDX analyses, showing the Pd-enrichment factor α defined by Eq. (1) against the Ni/Pd weight ratio in the initial Pd-Ni-C mixed powders

$$\alpha = \frac{(w_{Pd}/w_{Ni})_1}{(w_{Pd}/w_{Ni})_0}. \quad (1)$$

In this equation, α, w_{Pd}, and w_{Ni} correspond to the Pd-enrichment factor, Pd weight ratio in products, and Ni weight ratio in products, respectively, measured by EDX. The subscript symbols, 0 and 1, correspond to the initial mixed powders and the resulting products, respectively. It must be recognized that Pd is supposed to be enriched from the initial

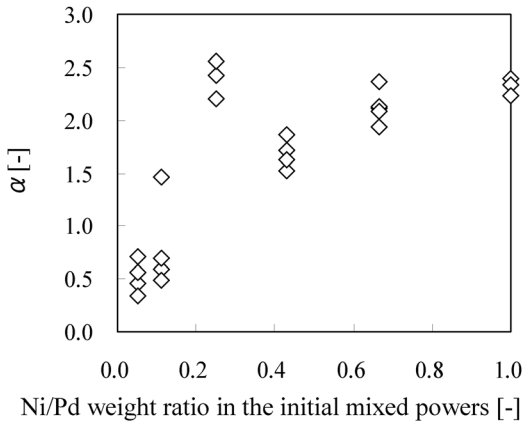

FIG. 6. Influence of Ni/Pd weight ratio in the initial Pd-Ni-C mixed powders on Pd-enrichment factor α determined by Eq. (1). Here, the Pd/C weight ratio was kept constant at 0.2.

mixtures to the produced alloy nanoparticles when α is higher than 1. Otherwise, Ni is enriched.

Overall, α tended to increase with the initial Ni/Pd weight ratio. As an important point, it was necessary for the initial Ni/Pd weight ratio to exceed a threshold in order to cause Pd enrichment. The value of α became lower than 1 when the initial Ni/Pd weight ratio was lower than approximately 0.1. The value of α was higher than 1 when the initial Ni/Pd weight ratio was higher than this threshold. The result suggests that Pd can be enriched by about a factor of two in the high Ni/Pd ratio range (from 0.28 to 1.0). It should be noted that the inverse of α corresponds to the Ni enrichment factor. When the Ni/Pd ratio was 0.05, the value of α became about 0.5. This means that Ni was enriched from the initial mixture to the products by about a factor of two.

The Pd-enrichment effect seen in the high Ni/Pd range could be explained by the condensation rates of Pd and Ni. Thermodynamically, the equilibrated vapor pressure at the gas-liquid interface of Pd is considered to be clearly lower than that of Ni when the vapors of Pd and Ni are liquidized into the nano-size liquid drops in the present reaction field. For example, such vapor pressures of Pd and Ni at 2900 K can be estimated to be 80.6 kPa and 99.6 kPa, respectively. (To obtain these values, the Clausius-Clapeyron equation[34] and the boiling points of Pd and Ni, which are 1555 and 1455 °C,[35] were used.) From this property, it is expected that Pd can be liquidized faster than Ni. This trend should be qualitatively preserved even when Pd and Ni coexist in the relevant reaction zone. These liquid drops may lead to the generation of solid alloy nanoparticles within the limited resident time in the cathode hole. Therefore, Pd can be enriched in the resulting alloy nanoparticles.

When the initial Ni weight ratio is fairly small, most of the Ni vapor could transfer to the resulting alloy nanoparticles. On the other hand, high-concentration Pd cannot completely condensate to nanoparticles in the cathode hole zone because its resident time there is too short. When the loss of Pd is much larger than that of Ni, Ni tends to be enriched. This Ni-enrichment effect may overcome the aforementioned Pd-enrichment effect when the Ni/Pd weight ratio is less than 0.1 in the present experiment.

Fig. 7 shows the influence of the weight ratio of the metallic components in the initial Pd-Ni-C mixed powders on α. Here, the Ni/Pd weight ratio was kept constant at 1.0 for all cases. It is shown that α increases with the metallic ratio, by which α changes from approximately 2 to 3. This result suggests that Pd can be enriched in these cases, and this enrichment effect can become more significant at the higher metallic ratio in the initial mixture.

C. Raman analysis on carbonaceous structures in SWCNHs dispersed with Pd-Ni alloy particles

It is common to evaluate the crystallinity of carbonaceous structures by Raman spectroscopy. An example of a Raman spectrum is shown in the inset of Fig. 8. Similar spectra were obtained from all the samples prepared in this study. Two distinctive peaks were seen in the spectrum. One peak around 1600 cm^{-1} is understood to indicate graphite structure, and another peak around 1350 cm^{-1} is understood to indicate defective structure.[36] Here, these peaks are referred to as the graphite peak (G peak) and the disorder peak (D peak), respectively. Fig. 8 shows the influence of the initial metallic weight ratio on the ratio of the intensity of the G peak to that of the D peak. This G/D ratio did not exhibit significant change even when the initial metallic ratio was varied from 0 to 0.57. From this result, it can be concluded that the carbonaceous structure in the SWCNHs dispersed with the alloy nanoparticles should not be affected by the metallic weight ratio. This analytical observation was consistent with TEM observations.

D. Dispersivity of SWCNHs with Pd-Ni alloy nanoparticles in ethanol

The as-grown powdery products of the SWCNHs with Pd-Ni alloy nanoparticles were dispersed in ethanol by sonication, and the diameter distribution of their discrete forms were evaluated by DLS. In this experiment, the Ni/Pd weight ratio in the initial Pd-Ni-C mixed powders was kept constant at 1.0, and the weight ratio of the metallic components in the initial mixture was varied. Fig. 9 shows the diameter distributions obtained from three ratios of the metallic

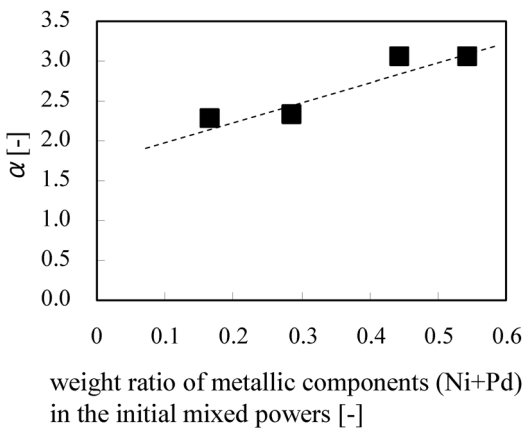

FIG. 7. Influence of the weight ratio of metallic components (Pd and Ni) in the initial Pd-Ni-C mixed powders on Pd-enrichment factor α determined by Eq. (1). Here, the initial Ni/Pd weight ratio was kept constant at 1.0.

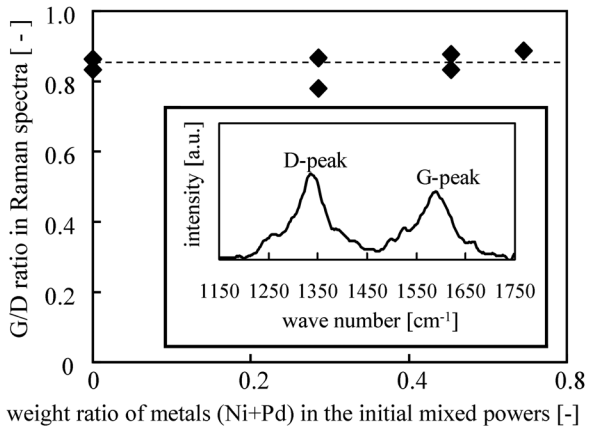

FIG. 8. The ratio of the graphite peak intensity to the disorder peak intensity (the G/D ratio) plotted against the weight ratio of metals (Ni and Pd) in the initial mixed power. Here, the Ni/Pd weight ratio was constant at 1.0. The inset shows an example of the Raman spectra, which was obtained for a metallic ratio of the initial mixed powders of 0.2.

components in the initial mixtures, 0.54, 0.28, and 0.16. It is shown that the alloy-dispersed SWCNHs form a sharper distribution of smaller aggregates when the ratio of the metallic components is increased. It is noticeable that this relationship between the metallic ratio in the initial mixture and the product particle sizes is opposite to the case of alloy nanoparticles shown in Fig. 4.

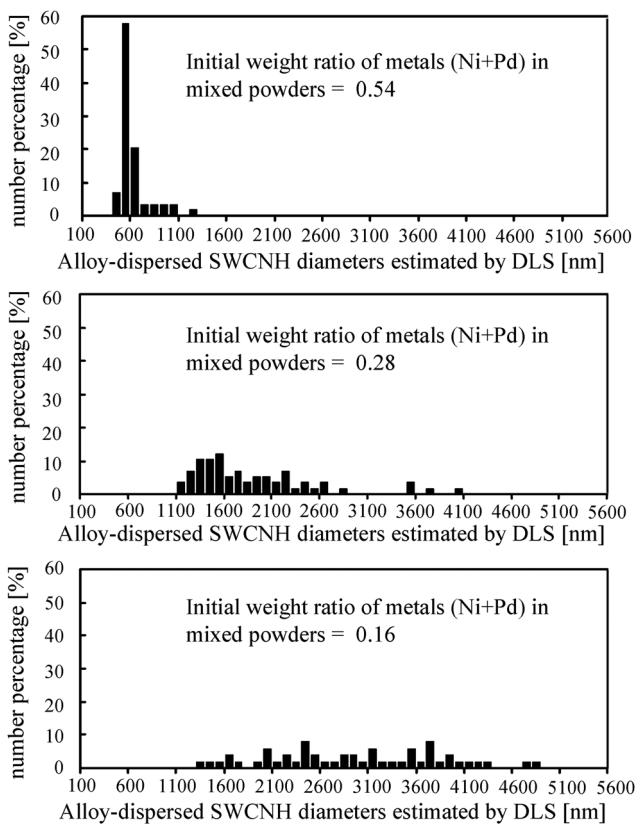

FIG. 9. Particle size distribution, obtained by DLS, of the discrete forms of SWCNHs dispersed with Pd-Ni alloy nanoparticles after sonication treatment. Here, the Ni/Pd weight ratio of the initial mixed powders was constant at 1.0, and the weight ratio of the metallic components (Pd and Ni) in the three histograms was set to 0.54, 0.28, and 0.16, respectively.

Note that the aggregation of SWCNHs is very rigid because a significant number of single C-C bonds in the SWCNH structures should prevent dispersal of SWCNH aggregates to individual primary horns.[37] Recently, primary horns were successfully isolated from the so-called dahlia-like SWCNHs by a partial combustion followed by a sucrose density gradient centrifugation.[38] However, even when such a special technique is applied, most of the SWCNH structures should still be aggregated forms, and simple sonication cannot lead to complete disassembling of SWCNHs. This is why the particle sizes shown in Fig. 9 are fairly large.

The mechanism of the effect of adding metallic components to the present reaction field to enhance the dispersion of SWCNHs in ethanol is not yet understood. There is a report about microscopic observation on core structures of SWNH aggregates synthesized by laser ablation, showing that the core of SWCNH aggregates consist of randomly stacked graphene sheets.[39] Thus, it can be inferred that higher dispersion of SWCNHs in any liquid needs either cores of smaller sizes or else the reduction of the abovementioned single C-C bonds between primary horns. The existence of relevant metallic vapor would hinder the growth of such cores and the generation of the single C-C bonds.

E. Comparison of sensitivities of H_2 sensors using SWCNHs dispersed with Pd-Ni alloy, Pd, and Ni nanoparticles

In TEM observation, the SWCNHs synthesized with Ni or Pd also had a similar structure to those dispersed with Pd-Ni alloy nanoparticles. The metal loading in the SWCNH aggregate was too low to measure in the present study. Nevertheless, the metal loading can be estimated by use of previous results obtained by arc discharge using a hollow graphite anode in which Pd wire of similar mass was inserted.[20] As a conclusion, the metal loading in case of SWCNHs having only Pd seemed to be 2–3 wt. %. In cases of Ni and Pd-Ni alloy, the metal loading might be relatively lower than this due to their boiling points which are lower than that of Pd.

Fig. 10 shows the change in the ohmic resistance of the SWCNH aggregate placed on the H_2 sensor caused by switching the gas components in the set-up described in Fig. 2. Here, the normalized change of the ohmic resistance defined by Eq. (2) is plotted against time

$$S = \frac{(R - R_0)}{R_0} \times 100. \tag{2}$$

In this equation, S, R, and R_0 correspond to the change of the normalized ohmic resistance plotted in Fig. 10, the absolute value of the ohmic resistance recorded at each time, and the initial value of the ohmic resistance, respectively. As shown in this figure, the resistance jumped up when the H_2-contained N_2 was introduced, and it decreased to the initial level when pure N_2 was fed afterward. It was observed that such behavior could be repeated more than 20 times stably. It was confirmed that the change in the ohmic resistance of the SWCNHs cannot be observed when the SWCNHs are not dispersed with any metallic component. Therefore, the

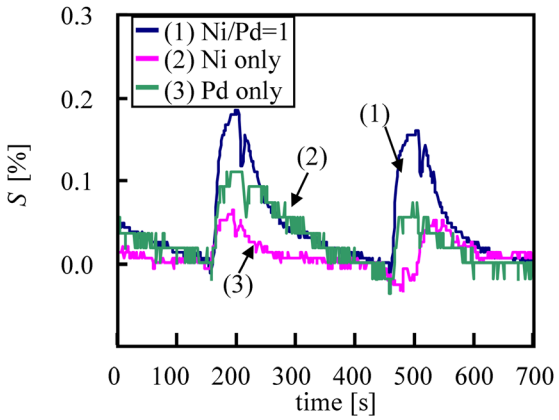

FIG. 10. The normalized change of ohmic resistance of SWCNH aggregate on the H_2 sensors fabricated with Pd-Ni alloy, Pd and Ni, defined by Eq. (2), when the set-up in Fig. 2 was used. The initial value of the ohmic resistance was controlled to be approximately 150 kΩ.

results observed in Fig. 10 suggest that SWCNHs dispersed with appropriate metallic components can be used to make H_2 sensors.

In comparison, SWCNHs dispersed with Pd-Ni alloy nanoparticles exhibited the highest sensitivity among the sensors used here. In Fig. 10, the change in the resistance obtained from SWCNHs with Pd-Ni alloy was about 3 times higher than that with Ni and about 1.5 times higher than that with Pd. It is widely known that Pd can be a useful material for fabricating H_2 sensors, and thus the SWCNHs dispersed with Pd can be expected to be used for H_2 sensors. The result obtained here indicates that alloying Pd with Ni can enhance the reactivity with H_2.

In our measurement, the value of the resistance should be governed by the resistance of the carbonaceous part of the SWCNHs because the volume of the carbonaceous part dominated that of the metallic part. It is known that H_2 can cause weak chemisorption onto a Pd surface,[27] and this interaction may constitute the origin of the sensitivity of Pd to H_2 at the Pd-based H_2 sensor. As SWCNHs can exhibit *p*-type semiconductive behavior for interaction from gas species,[25] the chemisorption of H_2 on a Pd surface would induce charge transfer from the metallic part to the carbonaceous part in SWCNHs. A similar mechanism would be expected when Ni is used. However, the reactivity of Ni to detect H_2 would be smaller than that of Pd in accordance with the present result. It is remarkable that Pd alloyed with Ni can exhibit the highest sensitivity to detect H_2, meaning that the charge transfer from the metallic particles to the carbonaceous part in SWCNHs should be accelerated by alloying.

It is expected that the sensitivity of the H_2 sensor can be increased if the Ni/Pd ratio is optimized in the alloying process. It must be noted that the syntheses of alloys in the products of the GI-AIW method have not yet been reported so far. Because the reactivity of the alloys dispersed in SWCNHs would be useful for many applications including the H_2 sensor, the information about the controllability of the structures and components in such products will be indispensable for achieving superior performance in any application. Due to this fact, investigation about the controlability of the structures and components of the products by varying synthesis conditions should be further pursued.

IV. CONCLUSIONS

SWCNHs dispersed with Pd-Ni alloy nanoparticles were synthesized in a one-step approach by the GI-AIW method using a hollow graphite rod anode charged with the mixed powders containing Pd and Ni. The TEM observation showed that the increase of metallic ratio in the initial powders led to the larger metallic particles. XRD indicated that the metallic nanoparticles dispersed in the products were Pd-Ni alloy, and the final component ratio depended on the Ni/Pd ratio in the initial powders. It was discovered by EDX analysis that Pd was enriched from the initial mixture to the products by a factor of two when the Ni/Pd weight ratio is relatively high, while Ni was enriched when the initial Ni/Pd ratio was lower than a threshold. Although the size and component ratio of the alloy nanoparticles depended on how much metallic components were added into the reaction field, the structural change of the carbonaceous part of the SWCNHs was not detected by Raman spectroscopy. The DLS result showed that the increase of the metallic components led to the higher dispersivity of SWCNHs in ethanol after sonication treatment. The knowledge gained here about the controllability of the structures and component ratios in the products will be essential for synthesizing high-performance SWCNHs dispersed with alloy nanoparticles. The H_2 sensor using the SWCNHs with Pd-Ni alloy nanoparticles exhibited higher sensitivity than that using Pd or Ni.

ACKNOWLEDGMENTS

This work is financially supported by Japan Society for the Promotion of Science (JSPS) Grant-in-Aid for Scientific Research B Contract No. 21360394.

[1]S. Iijima, M. Yudasaka, R. Yamada, S. Bandow, K. Suenaga, F. Kokai, and K. Takahashi, Chem. Phys. Lett. **309**, 165 (1999).
[2]T. Murakami, K. Ajima, J. Miyawaki, M. Yudasaka, S. Iijima, and K. Shiba, Mol. Pharmacol. **1**, 399 (2004).
[3]T. Yoshitake, Y. Shimakawa, S. Kuroshima, H. Kimura, T. Ichihashi, Y. Kubo, D. Kasuya, K. Takahashi, F. Kokai, M. Yudasaka, and S. Iijima, Physica B **323**, 124 (2002).
[4]N. Sano and S. Ukita, Mater. Chem. Phys. **99**, 447 (2006).
[5]K. Murata, J. Miyawaki, M. Yudasaka, S. Iijima, and K. Kaneko, Carbon **43**, 2826 (2005).
[6]E. Bekyarova, K. Kaneko, D. Kasuya, K. Murata, M. Yudasaka, and S. Iijima, Langmuir **18**, 4138 (2002).
[7]N. Sano, J. Phys. D: Appl. Phys. **37**, L17 (2004).
[8]N. Sano, J. Nakano, and T. Kanki, Carbon **42**, 686 (2004).
[9]C. Poonjarernsilp, N. Sano, H. Tamon, and T. Charinpanitkul, J. Appl. Phys. **106**, 104315 (2009).
[10]H. Takikawa, M. Ikeda, K. Hirahara, Y. Hibi, Y. Tao, P. A. Ruiz, Jr., T. Sakakibarak, S. Itoh, and S. Iijima, Physica B **323**, 277 (2002).
[11]M. Ikeda, H. Takikawa, T. Tahara, Y. Fujimura, M. Kato, K. Tanaka, S. Itoh, and T. Sakakibara, Jpn. J. Appl. Phys. **41**, L852 (2002).
[12]T. Yamaguchi, S. Bandow, and S. Iijima, Chem. Phys. Lett. **389**, 181 (2004).
[13]M. Schiavon, "Device and method for production of carbon nanotubes, fullerene and their derivatives" U.S. patent 7,125,525; EP 1,428,794.
[14]D. M. Gattia, M. V. Antisari, and R. Marazzi, Nanotechnology **18**, 255604 (2007).
[15]N. Li, Z. Wang, K. Zhao, Z. Shi, Z. Gu, and S. Xu, Carbon **48**, 1580 (2010).
[16]N. Sano, T. Kikuchi, H. Wang, M. Chhowalla, and G. A. J. Amaratunga, Carbon **42**, 95 (2004).

[17]N. Sano, T. Ishii, and H. Tamon, Carbon **49**, 3698 (2011).
[18]H. Kim, D. Lee, and J. Moon, Int. J. Hydrogen Energy **36**, 3566 (2011).
[19]Y. Jeong and T. T. M. Chung, Carbon **49**, 140 (2011).
[20]C. Poonjarernsilp, N. Sano, T. Charinpanitkul, H. Mori, T. Kikuchi, and H. Tamon, Carbon **49**, 4920 (2011).
[21]N. Sano, Carbon **43**, 450 (2005).
[22]N. Sano, Y. Kimura, and T. Suzuki, J. Mater. Chem. **18**, 1555 (2008).
[23]H. A. Pohl, *Dielectrophoresis: The Behavior of Neutral Matter in Nonuniform Electric Fields* (Cambridge University Press, Cambridge, UK, 1978).
[24]T. B. Jones, *Electromechanics of Particles* (Cambridge University Press, Cambridge, UK, 1995).
[25]J. Suehiro, N. Sano, G. Zhou, H. Imakiire, K. Imasakaa, and M. Hara, J. Electrost. **64**, 408 (2006).
[26]N. Sano, Y. Ikeyama, and H. Tamon, J. Chem. Eng. Jpn. **44**, 546 (2011).
[27]H. Nakatsuji, M. Hada, and T. Yonezawa, J. Am. Chem. Soc. **109**, 1902 (1987).
[28]I. V. Lebedeva, A. A. Knizhnik, A. V. Gavrikov, A. E. Baranov, B. V. Potapkin, S. J. Aceto, P.-A. Bui, C. M. Eastman, U. Grossner, D. J. Smith, and T. J. Sommerer, Carbon **49**, 2508 (2011).
[29]R. Löffler, M. Häffner, G. Visanescu, H. Weigand, X. Wang, D. Zhang, M. Fleischer, A. J. Meixner, J. Fortágh, and D. P. Kern, Carbon **49**, 4197 (2011).
[30]A. J. Page, S. Minami, Y. Ohta, S. Irle, and K. Morokuma, Carbon **48**, 3014 (2010).
[31]N. Sano, Chimica Oggi/Chem. Today **22**, 54 (2004).
[32]W. Si, G. Yu, Y. Ouyang, L. Tang, X. He, and B. Hu, J. Appl. Electrochem. **38**, 1727 (2008).
[33]D. J. Ham, C. Pak, G. H. Bae, S. Han, K. Kwon, S.-A. Jin, H. Chang, S. H. Choi, and J. S. Lee, Chem. Commun. **47**, 5792 (2011).
[34]P. W. Atkins, *Physical Chemistry*, 4th ed., Japanese version (Tokyo Kagaku Dojin, Tokyo, 1995).
[35]D. R. Lide, *Handbook of Chemistry and Physics*, 8th ed. (CRC, Boca Raton, 1999).
[36]T. Fujimori, K. Urita, Y. Aoki, H. Kanoh, T. Ohba, M. Yudasaka, S. Iijima, and K. Kaneko, J. Phys. Chem. C **112**, 7552 (2008).
[37]S. Utsumi, H. Honda, Y. Hattori, H. Kanoh, K. Takahashi, H. Sakai, M. Abe, M. Yudasaka, S. Iijima, and K. Kaneko, J. Phys. Chem. C **111**, 5572 (2007).
[38]M. Zhang, T. Yamaguchi, S. Iijima, and M. Yudasaka, J. Phys. Chem. C **113**, 11184 (2009).
[39]J. Xu, H. Tomimoto, and T. Nakayama, Carbon **49**, 2074 (2011).